JBC ARTICLE

Author's Choice

The Rho ADP-ribosylating C3 exoenzyme binds cells via an Arg–Gly–Asp motif

Received for publication, May 22, 2017, and in revised form, August 28, 2017 Published, Papers in Press, September 7, 2017, DOI 10.1074/jbc.M117.798231

Astrid Rohrbeck[‡1], Markus Höltje[§], Andrej Adolf[§], Elisabeth Oms[‡], Sandra Hagemann[‡], Gudrun Ahnert-Hilger[§], and Ingo Just[‡]

From the [‡]Institute of Toxicology, Hannover Medical School, Carl-Neuberg-Strasse 1, D-30625 Hannover and the [§]Institute of Integrative Neuroanatomy, Charité-Universitätsmedizin, D-10115 Berlin, Germany

Edited by Chris Whitfield

The Rho ADP-ribosylating C3 exoenzyme (C3bot) is a bacterial protein toxin devoid of a cell-binding or -translocation domain. Nevertheless, C3 can efficiently enter intact cells, including neurons, but the mechanism of C3 binding and uptake is not yet understood. Previously, we identified the intermediate filament vimentin as an extracellular membranous interaction partner of C3. However, uptake of C3 into cells still occurs (although reduced) in the absence of vimentin, indicating involvement of an additional host cell receptor. C3 harbors an Arg–Gly–Asp (RGD) motif, which is the major integrin-binding site, present in a variety of integrin ligands. To check whether the RGD motif of C3 is involved in binding to cells, we performed a competition assay with C3 and RGD peptide or with a monoclonal antibody binding to β1-integrin subunit and binding assays in different cell lines, primary neurons, and synaptosomes with C3-RGD mutants. Here, we report that preincubation of cells with the GRGDNP peptide strongly reduced C3 binding to cells. Moreover, mutation of the RGD motif reduced C3 binding to intact cells and also to recombinant vimentin. Anti-integrin antibodies also lowered the C3 binding to cells. Our results indicate that the RGD motif of C3 is at least one essential C3 motif for binding to host cells and that integrin is an additional receptor for C3 besides vimentin.

The family of bacterial C3[2] exoenzymes comprises eight ADP-ribosyltransferases of different origin (1–7). *Clostridium botulinum* C3 transferase (C3) is the prototype of this family. It is a single chain protein of ~25 kDa (8). C3 transfers an ADP-ribose moiety from NAD^+ to the small GTPases RhoA, RhoB, and RhoC at asparagine 41, whereby RhoA is the preferred substrate (9). C3 structurally lacks a translocation and binding domain and also the crystal structure of C3 does not give any hints how binding to cells and uptake is mediated (10, 11). It has been postulated that C3 exoenzymes are nonspecifically taken up by target cells, due to a high concentration of C3 and extended incubation time (12, 13). Fusion of C3 to various types of transport peptides was also used to circumvent the lack of the canonical uptake domain of bacterial protein toxins (14–16). However, we and others have shown that C3 from *C. botulinum* and *Clostridium limosum* efficiently enter different cells (neurons, astrocytes, neutrophils, and macrophages) at nanomolar concentrations and within short time periods (17–21). Recently, we demonstrated that C3 entered Chinese hamster ovary (CHO) cells within 10 min at a C3 concentration of 100 nM (22). Additionally, vimentin was identified as cell surface binding partner of C3 (23).

RGD (Arg–Gly–Asp) is the major integrin binding motif and the minimal peptide region known to interact with subsets of integrins. The integrin family is composed of 18 α and 8 β subunits that form up to 24 different heterodimers (24). These integrin receptors form N-terminal extracellular domains that bind ligands to mediate extracellular signals into the cell (25). Various ligands have been reported to use the RGD motif for cell entry, for instance: collagen (26), fibronectin (27), osteopontin (28), and TAT protein of HIV-1 (29). Integrins are also known to serve as receptors for pathogens like *Yersinia pseudotuberculosis* invasin (30, 31), Herpes simplex virus type 1 glycoprotein H (32), Epstein-Barr virus (33), and human cytomegalovirus (34). Integrins are anchored by a transmembrane domain and interact with diverse cytosolic proteins such as talin by a short cytoplasmic tail (35, 36) and with filamin (37–39). Compelling evidence suggests that integrins also interact with vimentin (40–44). β3 integrin is associated with vimentin thereby recruiting vimentin to the cell surface (45). Vimentin is an intermediate filament mediating cell adhesion, migration (46–48), wound healing (49), and cellular signaling (50). Recent studies suggest that surface vimentin plays a role in uptake of several pathogens (51–56). The exact molecular mechanism how vimentin reaches the extracellular site of the plasma membrane remained unclear. Additional to integrin, vimentin can associate with numerous other proteins such as actin (57), tubulin (58, 59), filamin (60), soluble CD44 (61), and insulin-like growth factor 1 receptor (IGF1R) (62).

We previously identified a role for vimentin in binding and uptake of C3 (21). Disruption of the vimentin network through acrylamide or depletion of intracellular vimentin by siRNA clearly reduces C3 uptake but does not completely block the

This work was supported by Deutsche Forschungsgemeinschaft (DFG) Grants JU 231/7-1 (to I. J.), RO 5129/2-1 (to A. R.), AH 67/10-1 (to G. A. H.), and HO 3249/5-1 (to M. H.). The authors declare that they have no conflicts of interest with the contents of this article.

This article contains supplemental Figs. S1–S4.

[1] To whom correspondence should be addressed: Carl-Neuberg-Str. 1, D-30625 Hannover, Germany. Tel.: 49-0-511-5322807; Fax: 49-0-511-5322879; E-mail: rohrbeck.astrid@mh-hannover.de.

[2] The abbreviations used are: C3, C3 exoenzyme derived from *Clostridium botulinum*; RGD, Arg–Gly–Asp; SARS, severe acute respiratory syndrome; ANOVA, analysis of variance; aa, amino acid(s).

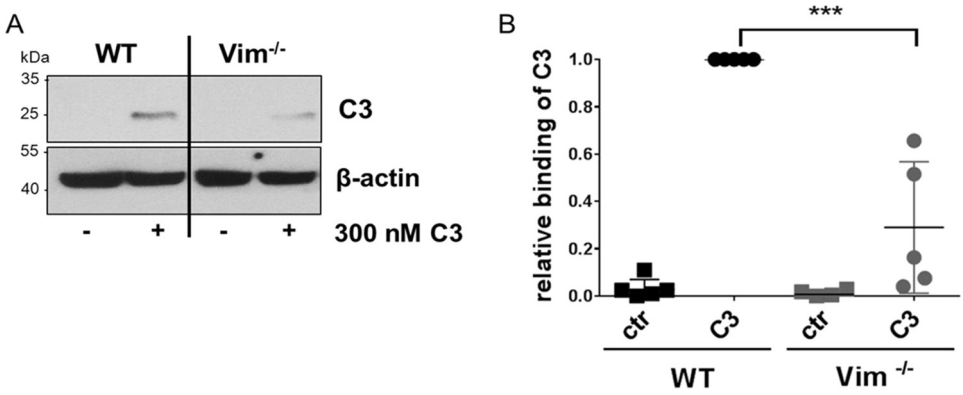

Figure 1. *A,* binding of C3 to intact primary vimentin-knock-out and wild-type neurons. Mixed hippocampal/neocortical neurons were exposed to 300 nM C3 for 1 h at 4 °C. Subsequently, cells were stringently washed three times, lysed, and submitted to Western blot analysis against C3 and β-actin. Western blots from representative experiments are shown ($n = 5$). *B,* diagram depicts densitometric evaluation of bound C3 and adjustment to the corresponding β-actin band. The signal intensity of bound C3 from C3-treated wild-type neurons was set as 1. Data represent the mean ± S.D. of five independent experiments. Statistical differences were determined by Student's *t* test (***, $p \leq 0.001$).

entry of C3 into cells (23). Recently, we showed in vimentin-knock-out neurons that vimentin is crucial for binding and uptake of C3 into neuronal cells (63). However, despite the complete lack of vimentin a weak signal of ADP-ribosylated RhoA/B was detected in vimentin-knock-out neurons. The extent of ADP-ribosylation was significantly reduced compared with the wild-type neurons but it was not completely inhibited. Additionally, application of extracellular vimentin to vimentin-knock-out neurons rescued the uptake of C3 and restored the growth-promoting effects of C3 (63). These findings suggested that C3 is able to bind to and enter cells via vimentin but another receptor appears to be involved.

In the present study we asked whether the RGD motif of C3 is relevant for its interaction with cell membranes. Indeed, we found that C3 binding to intact cells depends on the RGD motif. Moreover, results indicated that integrin and vimentin co-localized and interacted with each other. These findings suggest that integrin serves as a putative receptor for interacting with vimentin during C3 binding and uptake. Thus, both RGD motif and vimentin together with integrin are thought to mediate the uptake of C3.

Results

Reduced binding of C3 to vimentin-knock-out neurons

Recently, we showed that vimentin is involved in binding and uptake of C3 into cells (23, 63). In this context we examined whether C3 binds to vimentin-knock-out neurons. Therefore, intact vimentin-knock-out and wild-type neurons were exposed to 300 nM C3 for 1 h at 4 °C followed by stringent washing, lysis, and submission to Western blot analysis against C3bot. Interestingly, C3 also bound to the vimentin-free (knock-out) neurons (Fig. 1*A*), however, to a significantly reduced amount (Fig. 1*B*). Thus, binding of C3 to cells is mediated by vimentin and an additional structure. Therefore, we performed a ClustalW alignment of C3 exoenzymes to identify a putative common sequence motif for a binding site. Sequence alignment revealed that C3bot, C3cer, C3lim, and C3larvin contain an Arg–Gly–Asp (RGD) integrin recognition motif in their N-terminal residues (aa 88–90) (supplemental Fig. S1, *A* and *B*).

RGD peptide inhibits binding to and uptake of C3 into cells

Only a very limited quantity of neurons can be obtained from a single donor at one time and primary neurons cannot be expanded to large quantities, which are necessary for Western blot analysis. In addition, isolated primary neurons are often contaminated by astrocytes or glia cells. Thus, we used the immortalized murine hippocampal HT22 cell line as an alternative to primary neurons.

To investigate whether the RGD motif of C3bot is involved in binding and uptake into HT22 cells, a RGD competition assay was performed. Short synthetic peptides containing the RGD motif were used to inhibit binding to integrin (Fig. 2*A*). Binding of C3 to intact HT22 cells were competed by the G**RGD**NP peptide. A concentration of 100 μg/ml of G**RGD**NP peptide resulted in an approximate 50% displacement of C3 from the HT22 cells (Fig. 2*B*). Furthermore, preincubation of cells with G**RGD**NP peptide strongly inhibited internalization of C3 as evidenced by a diminished RhoA shift and decreased amount of ADP-ribosylated RhoA (Fig. 2, *C* and *D*). To confirm this finding, cells were pretreated with mAb D2E5, a monoclonal antibody that binds to the β1-integrin subunit followed by incubation with C3 for 1 h at 4 °C. Antibody treatment strongly reduced binding of C3 to intact cells (Fig. 2, *E* and *F*) and supported the findings of the competition assay with the RGD peptide.

Role of RGD motif in C3 binding to cells

The RGD sequence of C3 was mutated to RGG (D90G) or RGN (D90N) as well as RID (G89I). Because the arginine (Arg-88) residue of the RGD motif is important for the C3–NAD interaction (10, 64) this amino acid was not changed. The Asp-90 of the RGD motif forms a hydrogen bond to Arg-88 and therefore stabilizes the C3–NAD complex (10). Therefore, we performed two different Asp-mutant forms and converted the negatively charged Asp-90 to an uncharged Asn-90 or uncharged neutral Gly-90. No function of Gly-89 within the RGD motif has been reported.

Binding assays in three different cell types were performed to evaluate the influence of the RGD, RGN, or RID mutation in

C3 on cell binding. Notably, recognition of C3, C3-D90G, C3-D90N, and C3-G89I by α-C3bot was comparable (supplemental Fig. S2). Therefore, intact cells were exposed to increasing concentrations of C3 or C3-RGD mutants (10, 100, 500, and 1000 nM) for 1 h at 4 °C, followed by stringent washing, lysis, and submission to Western blot analysis against α-C3bot. Fig. 3, *A* and *B*, shows that C3 and the C3-RGD mutants bound to intact HT22 cells in a concentration-dependent manner. A significantly reduced binding of C3-RGD mutants compared with C3 wild-type was observed. Interestingly, the C3-D90G mutant bound less than the C3-G89I and C3-D90N mutants (Fig. 3*C*). The binding data were confirmed in macrophage-like cell line

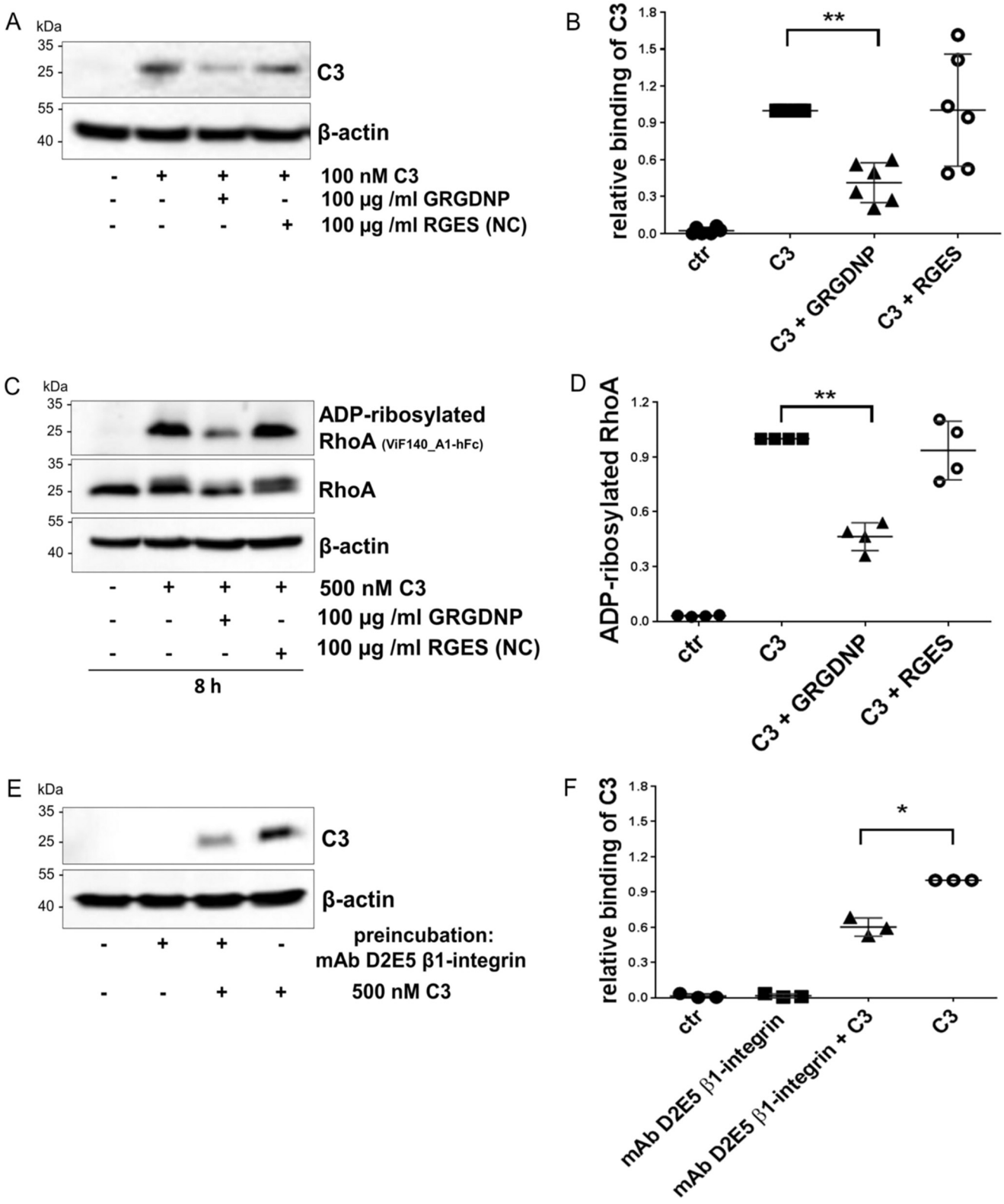

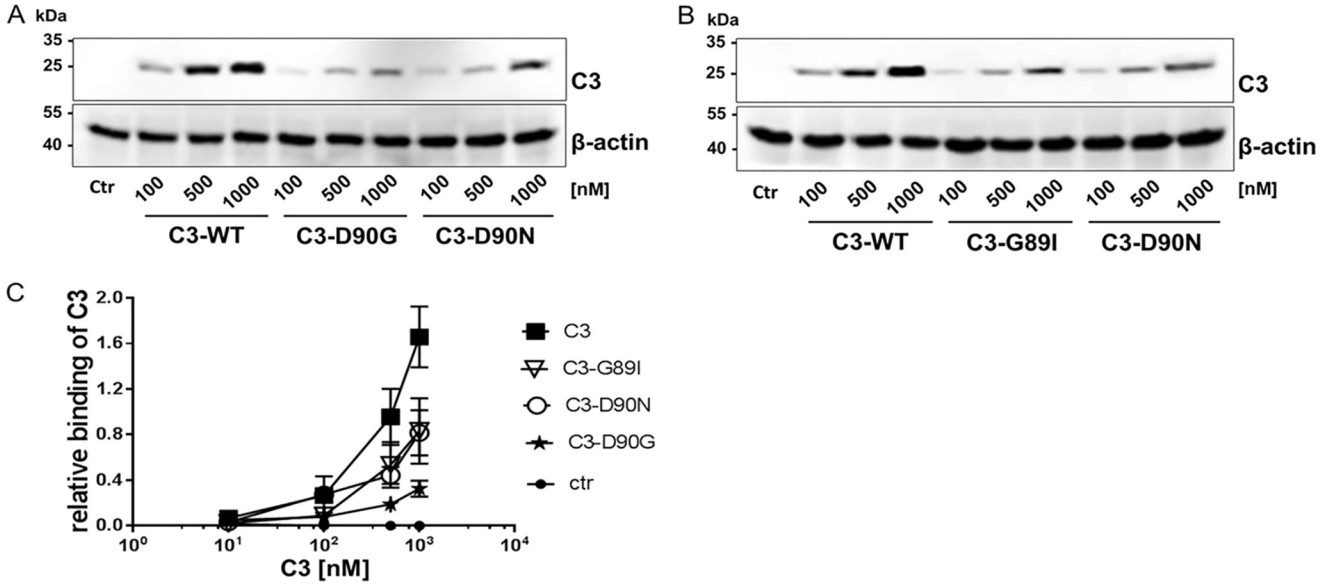

Figure 3. *A,* HT22 cells were exposed to increasing concentrations of C3 and C3-RGD mutants (C3-D90G and C3-D90N) and C3-G89I (*B*) for 1 h at 4 °C. Subsequently, cells were stringently washed three times, lysed, and submitted to Western blot analysis against C3 and β-actin. C3 and C3-D90N were analyzed in duplicates (*A* and *B*). *C,* diagram depicting densitometric evaluation of bound C3 and adjustment to the corresponding β-actin band ($n = 5$). Results represent the arithmetic mean ± S.D. of five independent experiments. Statistical differences between C3 and C3-RGD mutant-treated cells were determined by ANOVA and Dunnett's multiple *t* test. Results were statistically significant relative to C3 at a concentration of 500 and 1000 nM value, $p \leq 0.05$.

J774A.1 (supplemental Fig. S3, *A–C*) and also in hamster ovary CHO cells (supplemental Fig. S3, *D–F*). In both cell lines a strongly reduced binding of C3-RGD mutants compared with C3 was detected. Noteworthy, in hamster CHO cells the C3-G89I mutant bound weaker than the C3-D90N mutant. These findings indicate that the RGD motif of C3 is important for binding to intact cells.

Role of RGD motif in C3 binding to recombinant vimentin

In previous studies we showed that vimentin mediates binding and uptake of C3 into cells. To study whether the RGD motif of C3 is involved in binding to vimentin, recombinant vimentin was separated by SDS-PAGE followed by electroblotting onto nitrocellulose. The nitrocellulose was then overlaid with C3 or the C3-RGD mutants (C3-D90G, C3-D90N, or C3-G89I) followed by washing and detecting C3 by α-C3bot. Bound C3 was detected at a molecular mass of about 55 kDa (Fig. 4*A*, *arrow*). Binding of C3 seemed to be specific, because no signal was detected with BSA, which was loaded as negative control. Densitometric evaluation of bound C3 showed that wild-type C3 bound most strongly to vimentin, followed by C3-G89I, which bound about 45% less than C3. The substitution of asparagine at amino acid position 90 also caused a reduced binding capacity of C3-D90G and C3-D90N to vimentin (Fig. 4*B*). To rule out that any mutation in C3 *per se* altered the binding of C3 to vimentin, we performed the C3 overlay experiment with the enzyme-deficient C3-E174Q (supplemental Fig. S4*A*). In this assay the HT22 cell lysate served as positive control and showed that binding of C3-E174Q to the HT22 cell lysate and recombinant vimentin was similar to binding of C3 (supplemental Fig. S4*B*). To confirm this finding a reverse experiment was set up. C3 and C3-D90G, C3-D90N, and C3-G89I were separated by SDS-PAGE, blotted onto nitrocellulose membrane, and overlaid with His-tagged vimentin. After intensive washing the vimentin protein was visualized with an anti-His antibody (Fig. 5*A*). The loaded C3 were visualized using the C3bot antibody (Fig. 5*B*). Densitometric evaluation of bound His-tagged vimentin confirmed interaction between vimentin and C3, as well as C3-G89I and C3-G90N (Fig. 5*C*), however, with a reduced binding of vimentin to the C3-RGD mutants. Taken together, these results strongly indicate that the RGD motif is involved in binding of C3 to vimentin.

Figure 2. *A,* a competition assay with soluble RGD peptide revealed binding specificity of C3 to the RGD entity. HT22 cells were preincubated with 100 μg/ml of GRGDNP for 30 min at 4 °C followed by incubation with 100 nM C3 for 1 h at 4 °C. As negative control (*NC*) the RGES peptide was added. Subsequently, cells were stringently washed three times, lysed, and submitted to Western blot analysis against C3 and β-actin. Western blots from representative experiments are shown ($n = 6$). *B,* diagram depicts densitometric evaluation of bound C3 and adjustment to the corresponding β-actin band. The signal intensity of bound C3 from C3-treated cells was set as 1. Data represent the mean ± S.D. of six independent experiments. Statistical differences were determined by ANOVA and Dunnett's multiple *t* test (*, $p \leq 0.05$; **, $p \leq 0.01$). *C,* HT22 cells were preincubated with 100 μg/ml of GRGDNP for 30 min at 4 °C followed by incubation with 500 nM C3 for 8 h at 37 °C. Subsequently, cells were stringently washed three times, lysed, and submitted to Western blot analysis against RhoA, ADP-ribosylated RhoA, and β-actin. The signal intensity of ADP-ribosylated RhoA from C3-treated cells (without preincubation) was set as 1. Western blots from representative experiments are shown ($n = 4$). *D,* densitometric analysis of (*C*) ADP-ribosylated Rho antibody is shown. Data represent the mean ± S.D. of four independent experiments. Statistical differences were determined by ANOVA and Dunnett's multiple *t* test (*, $p \leq 0.05$; **, $p \leq 0.01$). *E,* HT22 cells were preincubated with 3 μl/ml of mAb D2E5 to the β1-integrin subunit for 30 min at 4 °C followed by incubation with 500 nM C3 for 1 h at 4 °C. Subsequently, cells were stringently washed three times, lysed, and submitted to Western blot analysis against C3 and β-actin. Western blots from representative experiments are shown ($n = 3$). *F,* diagram depicts densitometric evaluation of bound C3 and adjustment to the corresponding β-actin band. The signal intensity of ADP-ribosylated RhoA from C3-treated cells (without preincubation with the antibody) was set as 1. Data represent the mean ± S.D. of three independent experiments. Statistical differences were determined by ANOVA and Dunnett's multiple *t* test (*, $p \leq 0.05$).

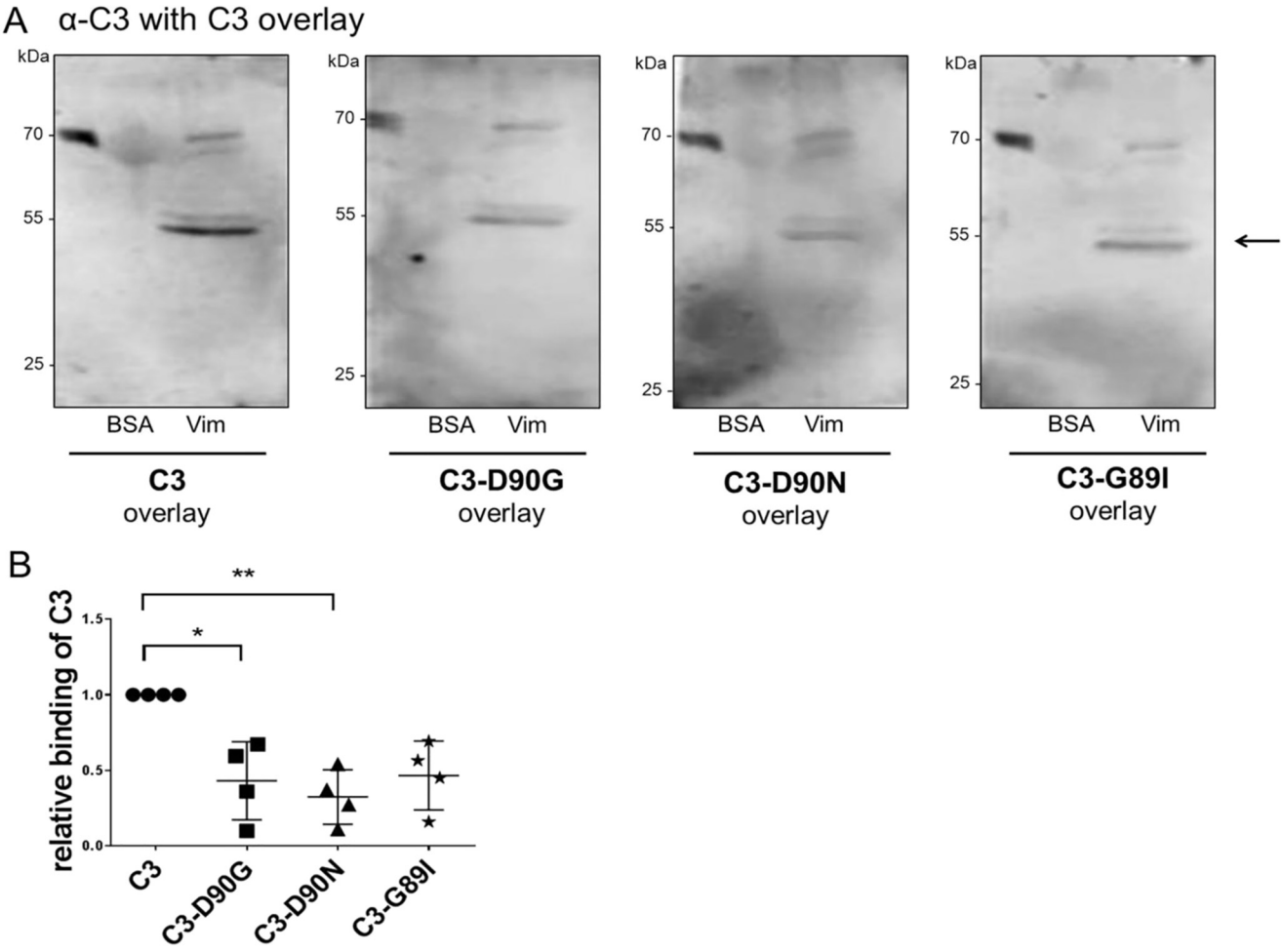

Figure 4. *A,* C3 overlay (binding of C3 to vimentin). Recombinant vimentin (35 μg) was purified as described under "Experimental procedures" followed by separation through SDS-PAGE and transfer onto nitrocellulose. Nitrocellulose was incubated with 10 μg/ml of C3 or C3-RGD mutants (as indicated) for 1 h at 4 °C. After washing, bound C3 was detected by anti-C3. BSA was used as negative control. *B,* diagram depicts densitometric evaluation of bound C3 and adjustment to the 70-kDa reference band of the protein ladder ($n = 4$). The signal intensity of bound C3-WT was set as 1. Data represent the mean ± S.D. of four independent experiments. Statistical differences were determined by ANOVA and Dunnett's multiple *t* test (*, $p \leq 0.05$; **, $p \leq 0.01$).

To study if the amino acid substitutions within the RGD motif impair the ability of C3 to ADP-ribosylate RhoA we performed an *in vitro* sequential [^{32}P]ADP-ribosylation assay with recombinant RhoA. The enzyme activity of all three C3-RGD mutants was significantly reduced (data not shown), which hampers the statement about the uptake of the C3-RGD mutants.

Synaptosomes

To confirm that β1-integrin is involved in binding of C3 to cells, we conducted further experiments using synaptosomes prepared from postnatal mouse whole brains. Western blotting detected the presynaptic marker protein synaptophysin enriched in synaptosomes compared with whole brain homogenate and postnuclear supernatant. Also, β1-integrin was detected in synaptosomes at significantly higher levels. The intermediate filament protein vimentin, which is expressed in adult brains mainly in glial cells but not in neurons, was detected in the homogenate and postnuclear supernatant but not in synaptosomes (Fig. 6*A*). Both the lack of vimentin and the absence of glial fibrillary acidic protein hardly detectable in young postnatal (P2) brains indicated a successful depletion of the synaptosomal fraction from glial constituents. Therefore, synaptosomes represent a suitable purified neuronal model to evaluate the binding of C3 to integrin. Despite the lack of vimentin, C3 bound to synaptosomes and confirmed the observed binding of C3 to vimentin-knock-out neurons (see Fig. 1). Substitution of Gly of the RGD motif resulted in strong reduction of C3-G89I binding to synaptosomes (Fig. 6, *B* and *C*). This finding supports the notion that the RGD motif is involved in binding of C3 to cells including neurons. Notably, a direct comparison of the influence of vimentin on C3-binding is not possible, because synaptosomes do not contain vimentin.

Reduced binding of His-C3stau2 to cells compared with His-C3bot

Sequence alignment revealed that all three isoforms of C3stau harbor instead of the RGD motif a RGD-like motif, Arg–Leu–Asp (RLD aa 70–72) sequence, which is recognized by $\alpha v\beta 3$ and $\alpha_M\beta 2$ integrins (65, 66). Additionally, C3stau contains a LLNLD (aa 89–93) sequence (supplemental Fig. S1, *A* and *C*), which is consistent with the integrin α subunit recognition consensus (67) and represents a clathrin box motif (68). To investigate the C3 cell interaction further, a His-tagged form

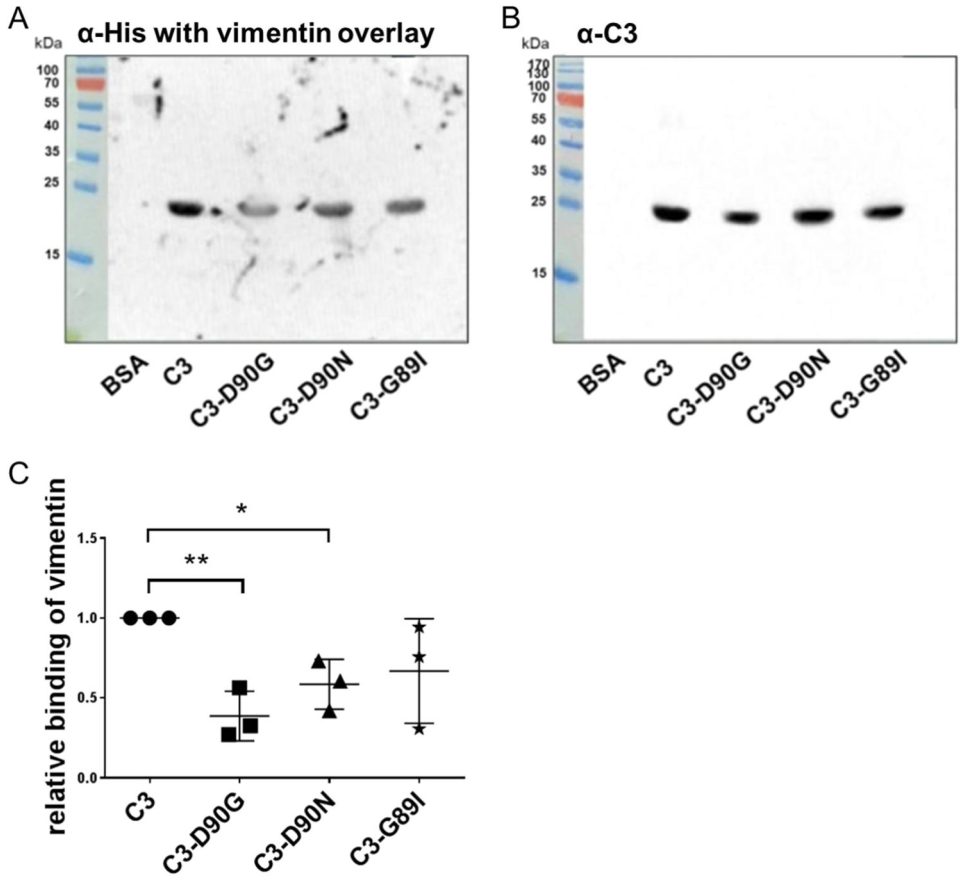

Figure 5. *A,* binding of vimentin to C3 or C3-RGD mutants (as indicated). Purified C3 (4 μg) or C3-RGD mutants (4 μg) were separated through SDS-PAGE and transfered onto nitrocellulose. Nitrocellulose was incubated with 10 μg of His-tagged vimentin for 60 min at 4 °C. After washing, bound vimentin was detected by penta-His polyclonal antibody. BSA was used as negative control. *B,* Western blot of loading C3 samples is shown. *C,* diagram depicts densitometric evaluation of bound vimentin and adjustment to the corresponding band in the α-C3 Western blot ($n = 3$). The signal intensity of bound His-tagged C3-WT was set as 1. Data represent the mean ± S.D. of three independent experiments. Statistical differences were determined by ANOVA and Dunnett's multiple *t* test (*, $p \leq 0.05$; **, $p \leq 0.01$).

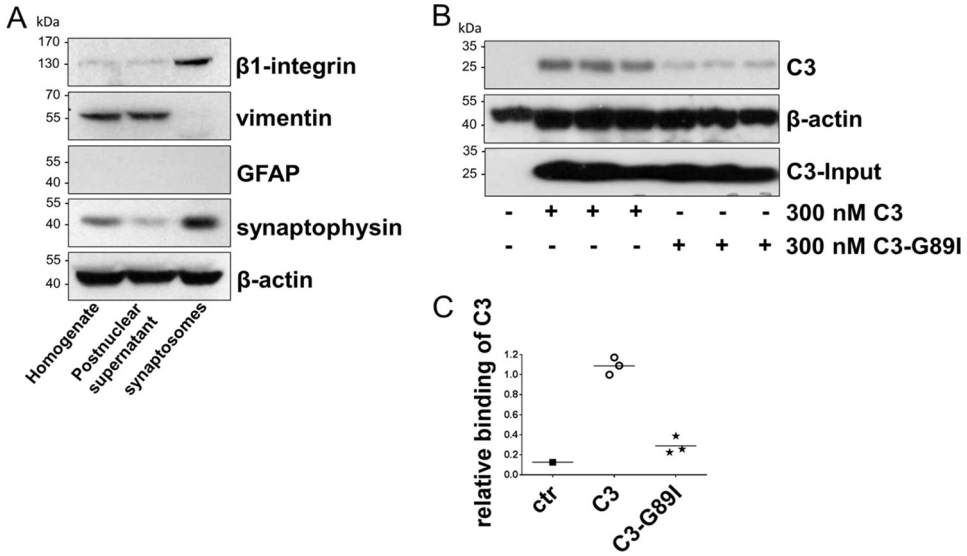

Figure 6. *A,* total protein (20 μg) from mouse brain homogenates, postnuclear supernatant, and synaptosome suspension were prepared and submitted to Western blot analysis against the synaptic protein synaptophysin, β1-integrin, the intermediate filaments vimentin and glial fibrillary acidic protein (*GFAP*). β-Actin served as a loading control. *B,* synaptosomes were incubated with 300 nM C3 or C3-G89I for 1 h at 4 °C. Subsequently, synaptosomes were stringently washed, lysed, and submitted to Western blot analysis against C3 and β-actin. *C,* binding of C3 is shown as means of three biological triplicates ($n = 1$). Bound C3 was densitometrically evaluated and adjusted to the corresponding β-actin and C3-input band.

of the C3bot and C3stau2 exoenzymes was used (His-tagged C3 proteins were used due the lack of a suitable antibody recognizing both C3bot and C3stau2 at comparable affinities). To investigate binding of the C3 exoenzymes to HT22 cells, identical amounts of His-C3bot or His-C3stau2 were added to cells for 1 h at 4 °C. Significant differences between His-C3bot and His-

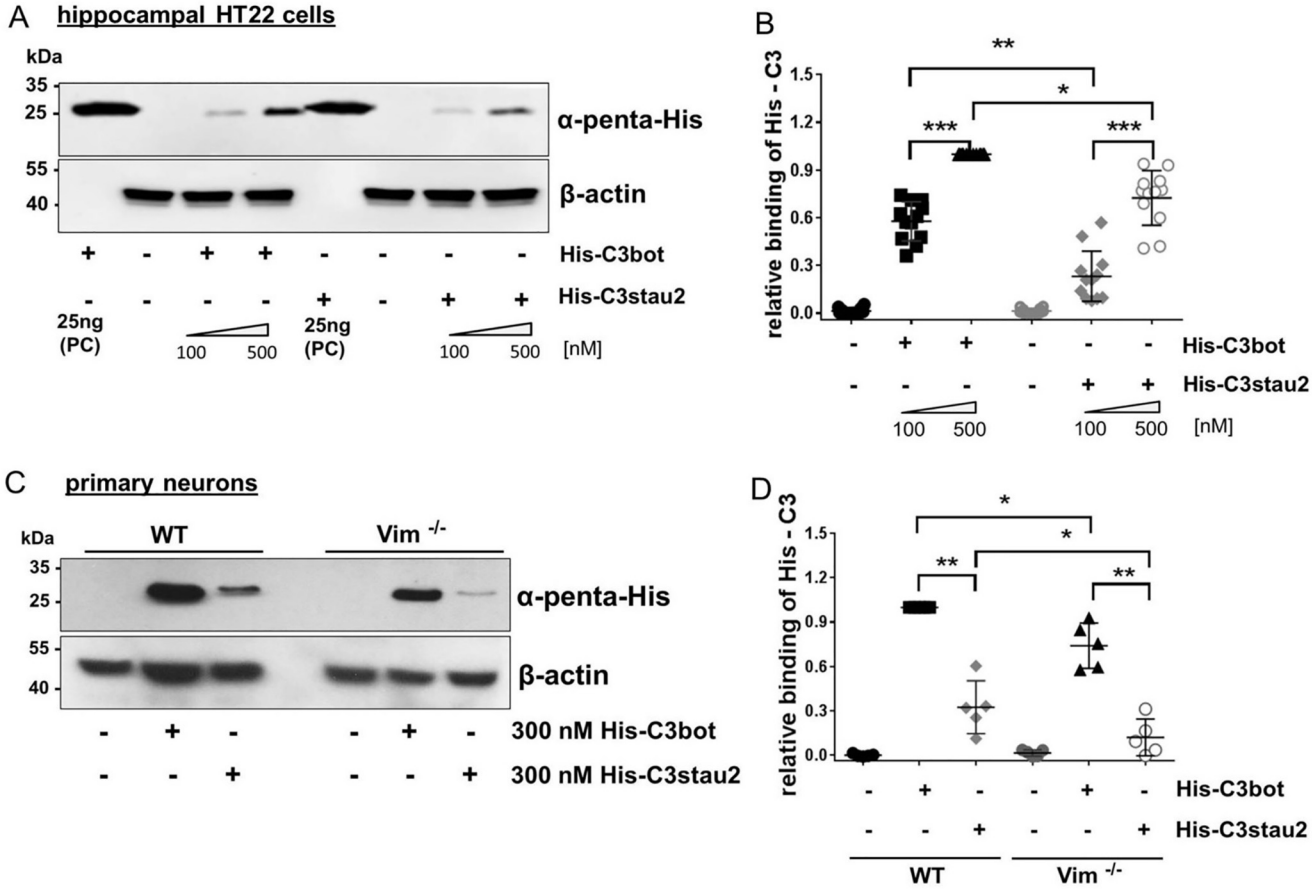

Figure 7. *A,* binding of His-C3bot and His-C3stau2 to intact hippocampal HT22 cells. Cells were exposed to 100 or 500 nM His-C3bot or His-C3stau2 for 1 h at 4 °C. Subsequently, cells were stringently washed three times, lysed, and submitted to Western blot analysis against penta-His and β-actin. Western blots from representative experiments are shown ($n = 5$). *PC,* positive control, 25 ng of His-C3bot or His-C3stau2 in 5× Laemmli buffer. *B,* diagram depicts densitometric evaluation of bound His-tagged C3 and adjustment to the corresponding β-actin band. The signal intensity of bound His-C3 from 500 nM His-C3bot-treated HT22 cells was set as 1. Data represent the mean ± S.D. of five independent experiments with biological duplicates. Statistical differences were determined by ANOVA and Dunnett's multiple *t* test (*, $p \leq 0.05$; **, $p \leq 0.01$; ***, $p \leq 0.001$). *C,* binding of His-tagged C3 to intact primary vimentin-knock-out and wild-type neurons. Mixed hippocampal/neocortical neurons were exposed to 300 nM His-C3bot or His-C3stau2 for 1 h at 4 °C. Subsequently, primary neurons were stringently washed, lysed, and submitted to Western blot analysis against penta-His and β-actin. *D,* diagram depicts densitometric evaluation of bound His-tagged C3 and adjustment to the corresponding β-actin band. The signal intensity of bound His-C3 from 300 nM His-C3bot-treated wild-type neurons was set as 1. Data represent the mean ± S.D. of five independent experiments. Statistical differences were determined by ANOVA and Dunnett's multiple *t* test (*, $p \leq 0.05$; **, $p \leq 0.01$).

C3stau2 binding to cells were observed. His-C3stau2 binding to HT22 cells was reduced compared with binding of His-C3bot (Fig. 7*A*). Binding of His-C3stau2 to HT22 cells was ~60% of the binding of His-C3bot (Fig. 7*B*). In addition, a reduced binding of His-C3stau2 in primary cells was detected (Fig. 7*C*). Moreover, vimentin mediates binding of both His-C3bot and His-C3stau2 because the amount of bound His-C3 to vimentin-knock-out neurons was significantly reduced compared with wild-type neurons. Finally, a reduced binding of His-C3stau2 compared with His-C3bot was detected in vimentin-knock-out neurons (Fig. 7*D*). These differences suggest that the altered binding site of C3stau2 might result in reduced binding affinity.

Discussion

Previous studies have revealed that vimentin is involved in binding and uptake of C3bot (23). However, findings indicate that alternative or additional binding partners besides vimentin may exist. First, although vimentin was successfully reduced by siRNA, binding and uptake of C3bot was not completely inhibited. Second, in C3 overlay-binding assays several positive spots were detected containing other proteins than vimentin. Third, as shown in Figs. 1, 6*B,* and 7*C* despite the lack of vimentin, C3 binds to vimentin-knock-out neurons and vimentin-free synaptosomes. To identify additional binding partners via binding consensus sequences or binding motifs in C3 we performed sequence alignment analyses of different C3 isoforms and found the RGD motif in all C3 exoenzymes with the exception of C3stau. The RGD motif is the cell attachment site of a large number of adhesive extracellular matrix, blood, and cell surface proteins, and known integrins (αvβ1, αvβ3, αvβ5, αvβ8, and α5β1) recognize this sequence. Studies have shown that many pathogens use different types of RGD-recognizing integrin receptors (αvβ1, αvβ3, αvβ6, and αvβ8) to bind to and enter the host cells (69–72). The RGD motif has also been found in bacterial protein toxins. For example, the α-toxin of *Staphylococcus aureus* interacts with β1-integrin of epithelial cells (73). The *Streptococcus pyogenes* pyrogenic exotoxin B binds to αvβ3 or α2bβ3 integrins on endothelial cells and platelets (74). The role and importance of the RGD motif in binding of C3 to cells has been investigated by competition-binding studies. The

competitive inhibition experiments using the G**RGD**NP peptide and preincubation of cells with an antibody against β1-integrin remarkably decreased the binding of C3 to HT22 cells. This indicates that the RGD motif is crucial for effective interaction between C3 and HT22 cells. Additionally, mutations in the RGD motif of C3 (such as Asp-90 and Gly-89) led to reduced binding of C3 to different cell lines. But the replacement of this amino acid also leads to significant loss of enzymatic activity as this motif is also involved in binding to the cosubstrate NAD^+.

Furthermore, compelling evidence suggests that integrins associate with vimentin. The αvβ3 and α2β1 integrins bind to vimentin through integrin-associated proteins (41). In primary microvascular endothelial cells fibrinogen-associated αvβ3 integrin was assembled in structures harboring vimentin filaments (42). In CHO cells Bhattacharya and co-workers (45) demonstrated a close association between β3 integrin and vimentin at the basal surface of the cell. Moreover, they showed that integrin regulates interaction of vimentin with the cell surface. Recently, it was also shown that vimentin filaments underneath the plasma membrane directly interact with integrin tails and cause integrin clustering and enhanced integrin-mediated cell adhesion (44). Integrins are transmembrane cell adhesion receptors; therefore the interaction between vimentin and integrin takes place near the plasma membrane. From these data we suggest that vimentin from the plasma membrane region interacts with integrin. Interestingly, vimentin contains an Arg–Leu–Asp (RLD) motif within the rod1b domain (aa 217–219). RLD is a binding motif for integrins αvβ3 and $\alpha_M\beta2$ (65, 69, 75). Based on this finding an extracellular interaction between vimentin and integrin appears feasible. In a previous study the rod domain of vimentin was identified as a binding partner of C3 (23). Vimentin at the cell surface has been reported in several studies (23, 76–80). Vimentin is involved in binding and uptake of several pathogens (51–54, 81, 82). Recently, a further study has shown that surface vimentin is a co-receptor for SARS-coronavirus (56). Moreover, findings indicated that vimentin is one of the interacting partners of the ACE2 receptor (the identified functional receptor for SARS-coronavirus, (83)) and directly binds to the SARS-coronavirus spike protein. Vimentin also mediates the entry of SARS-coronavirus (56). In this context, it is known that in addition to integrins, other proteins or receptors served as co-receptor and were involved in cell entry of pathogens. For example, both integrins (α3β1 and α9β1) and ephrin receptor tyrosin kinase A2 serve as receptors for Kaposi's sarcoma-associated herpesvirus (84–86). Like Kaposi's sarcoma-associated herpesvirus, adenovirus type 2 uses coxsackievirus and adenovirus receptor (CAR) and αvβ3/αvβ5 integrins for productive entry (87, 88). Furthermore, reovirus binds first to its cell attachment factor sialic acid (89) and then to its co-receptor β1 integrin (90). This interaction drives the recruitment and clustering of the junctional adhesion molecule A and caused internalization of the virus–receptor complex (91, 92). However, both vimentin and integrin have been shown to act as direct receptor and co-receptor and both are involved in endocytosis. Therefore, it is conceivable that vimentin and integrin also act together. This is supported by the findings of Yang and co-worker (93), they described that the rod domain of superficial vimentin is involved in binding and uptake of dengue virus. Previously it was shown that β3 integrin was required for dengue virus serotype 2 infection (94). Therefore it was postulated that dengue virus uses more than one receptor to infect cells and that perhaps β3 integrin and superficial vimentin cooperate in mediating dengue virus infection (93).

The involvement of the RGD motif in binding to cells is clear. As mutations within the RGD motif of C3 cause loss of enzyme activity, no study of the role of the RGD motif in the uptake of C3 can be performed. In conclusion, the RGD motif in C3 is crucially involved in its binding to cells, as even conservative changes to RGG, RGN, or RID significantly reduced the binding capacity of C3. The RGD motif mediates direct binding of C3, to recombinant vimentin as well as to integrin (synaptosomes, $Vim^{-/-}$ neurons). Moreover, His-C3bot binding to cells was significantly enhanced compared with His-C3stau2, which lacks the RGD motif. C3bot harbors only one RGD motif implicating binding to either vimentin or integrin. However, a complex between vimentin and β1 integrin may enhance the C3bot binding. How the interaction of vimentin with integrin is regulated by C3 is still unclear. But all three players must cooperate as addition of vimentin to vimentin-knock-out neurons (harboring integrin) enhances strong binding and uptake of C3bot (63).

Experimental procedures

Cell culture

Murine hippocampal HT22 cells, which were a generous gift from Prof. Dr. Carsten Culmsee (Institute for Pharmacology and Toxicology, Philipps University Marburg, Germany) (95), were cultured in Dulbecco's modified essential medium (Biochrom, + 10% FCS, 1% penicillin, 1% streptomycin, and 1 mM sodium pyruvate). J774A.1 mouse macrophages (purchased from American Type Culture Collection ATCC: TIB-67) were cultivated in RPMI 1640 medium (Biochrom; with 10% FCS, 1% penicillin, 1% streptomycin, and 1 mM sodium pyruvate). Cells were maintained at 37 °C and 5% CO_2. Upon confluence, cells were passaged. Wild-type Chinese hamster ovary cells (CHO-K1, ATCC: CCL-61, which were a generous gift from Prof. Dr. Gerardy-Schahn (Institute for Cellular Chemistry, Hannover Medical School, Germany) were cultivated in Dulbecco's modified essential medium/Ham's F-12 medium (Biochrom; with 10% fetal bovine serum, 1% penicillin, 100 units/ml of streptomycin, and 1 mM sodium pyruvate). Cells were maintained at 37 °C and 5% CO_2. Upon subconfluence, cells were passaged. Neurons were obtained from fetal NMRI (hippocampus culture) or 129 SVEV wild-type and 129 SVEV $Vim^{-/-}$ knock-out mice (mixed hippocampal/neocortical culture) at embryonic day 16 (E16) as described before (63).

Synaptosomes were prepared at 4 °C from postnatal (P2) mouse whole brains in the presence of protease inhibitors according to a modified standard procedure as described (96). Briefly, after homogenization in 0.32 M sucrose (10 strokes at 900 rpm) and centrifugation at 1,300 × *g* for 10 min, the supernatants were centrifuged at 14,000 × *g* for 15 min. Crude syn-

aptosomes (1–2 mg of protein) were dissolved in PBS and incubated with C3 or C3-G89I.

RGD competition assay

For the RGD competition assays cultured HT22 cells were seeded onto 3.5-cm plates at a concentration of 300,000 cells/ml and grown for 24 h at 37 °C and 5% CO_2. The medium was removed and cells were washed with PBS. HT22 cells were preincubated with 100 μg/ml of G**RGD**NP for 30 min at 4 °C followed by incubation with 100 nM C3 for 1 h at 4 °C. As negative control the RGES peptide was added. Cells were washed and scraped into Laemmli sample buffer. The obtained suspension was shaken at 37 °C for 10 min. Ultrasonic disruption was performed in a cycle of 10 × 5 s, 5 × 10% sonic energy using a sonotrode (Bandelin Electronic, Berlin, Germany). The lysate was then incubated at 95 °C for 10 min and submitted to SDS-PAGE and Western blot analysis against α-C3 and β-actin.

Expression and purification of recombinant C3 protein

C3 wild-type and *C. botulinum*-derived mutant C3-E174Q (carrying a point mutation from glutamate to glutamine at amino acid 174) were expressed as recombinant GST fusion proteins in *Escherichia coli* TG1 harboring the respective DNA fragment (gene of *C. botulinum* C3, accession number X59039) in plasmid pGEX-2T (GE Healthcare Europe GmbH, Freiburg, Germany) as described previously. Briefly, pGEX-2T plasmids encoding wild-type or enzyme-deficient C3bot were transformed into *E. coli* TG1 cells. Starter cultures grown in Luria-Bertani broth with ampicillin at 37 °C overnight were diluted into fresh media. Cells were grown for 3 h (A_{600} = 0.7) at 37 °C, isopropyl 1-thio-β-D-galactopyranoside was added to a final concentration of 200 μM to induce the C3bot expression for another 3 h. Cells were harvested by centrifugation, resuspendend in lysis buffer (20 mM Tris-HCl, pH 7.4, 10 mM NaCl, 5 mM $MgCl_2$, 5 mM DTT, and 1 mM PMSF), and lysed ultrasonically (3 × 20 s, 90% cycle, 20% power) on ice. The lysate was centrifuged for 30 min at 15,000 × *g*. The supernatant was incubated with glutathione-Sepharose beads for 5 h at 4 °C to bind the GST fusion protein. Beads were washed with buffer containing 50 mM Tris-HCl (pH 8.0), 10 mM glutathione, 100 mM NaCl and PMSF. The GST-fused C3bot protein was cleaved from the beads with thrombin (Sigma, Berlin, Germany) in a buffer containing 50 mM Tris-HCl (pH 8.0), 50 mM NaCl, and 2.5 mM $CaCl_2$. Purified proteins were then concentrated to 1 ml with a Centricon microconcentrator (Amicon, Danvers, MA) with a 30,000 molecular weight cutoff. Thrombin was removed from purified C3bot by use of *p*-aminobenzamidine beads (Sigma). Buffer exchange was performed by use of PD 10 column (GE Healthcare, Europe GmbH, Freiburg, Germany) and purified C3bot was eluted in 20 mM HEPES (pH 7.5). Eluted proteins were analyzed by 15% SDS-PAGE and stained with Coomassie Blue. ADP-ribosyltransferase activity was measured by an *in vitro* ADP-ribosylation assay.

Generation of C3-RGD mutants by site-directed mutagenesis

Individual substitution of asparagine or glycine residues within the RGD motif of C3bot were introduced using QuikChange II XL site-directed mutagenesis kit, according to the manufacturer's instructions (Agilent, Santa Clara, CA). The primers used were as follows: forward, D90G_For (5′-ATGTTATTTAGAGGCGGCGACCCTGCTTATTTAGG-3′), and reverse, D90G_Rev (5′-CCTAAATAAGCAGGGTCGCCGCCTCTAAATAACAT-3′), D90N_For (5′-ATGTTATTTAGAGGCAACGACCCTGCTTATTTAGG-3′), and reverse, D90N_Rev (5′-CCTAAATAAGCAGGGTCGTTGCCTCTAAATAACAT-3′), and G89I_For (5′-ATGTTATTTAGAATCGACGACCCTGCTTATTTAGG-3′), and reverse, G89I_Rev (5′-CCTAAATAAGCAGGGTCGTCGATTCTAAATAACAT-3′). Correct nucleotide sequences were confirmed by sequencing.

Expression and purification of His-tagged recombinant C3 proteins

C3bot (gene of *C. botulinum* C3, accession number X59039) and C3stau2 (gene of *Staphylococcus aureus* C3, accession number AJ277173) cDNA constructs were successfully cloned into pQE-30 vector (Qiagen), with the N-terminal His tag. The recombinant constructs were transformed into *E. coli* TG1 and grown in 1-liter volumes of LB medium. The cells were grown to an A_{600} of 0.6 and induced with 200 μM isopropyl 1-thio-β-D-galactopyranoside for 3 h. Cells were collected by centrifugation (5,000 rpm for 20 min) and kept at −20 °C overnight. The frozen cells were later thawed, resuspended with 50 ml of lysis buffer (50 mM NaH_2PO_4, 300 mM NaCl, and 10 mM imidazole), disrupted using a French press, and centrifuged at 15,000 rpm for 20 min. The resultant supernatant was incubated for 30 min on ice with DNase (10 μg/ml) and loaded onto a Talon metal affinity column (BD Biosciences Clontech, BD Biosciences). Bound His-tagged C3 protein was eluted with elution buffer (50 mM NaH_2PO_4, 300 mM NaCl, and 250 mM imidazole, adjust to pH 8.0). Buffer exchange was performed by use of PD 10 column (GE Healthcare, Europe GmbH) and purified His-tagged C3 was eluted in 20 mM HEPES (pH 7.5). Eluted proteins were analyzed by 15% SDS-PAGE and stained with Coomassie Blue. ADP-ribosyltransferase activity was measured by an *in vitro* ADP-ribosylation assay. Protein concentrations were determined using the NanoDrop ND-1000 spectrophotometer.

C3 binding assay

For the binding assays cultured cells were seeded onto 3.5-cm plates at a concentration of 300,000 cells/ml and grown for 24 h at 37 °C and 5% CO_2. The medium was removed and cells were washed with PBS. 300,000 cells/ml were exposed to 10, 100, 500, or 1000 nM C3 or C3-RGD mutants for 1 h at 4 °C. Subsequently, cells were stringently washed three times with PBS. Cells were scraped into Laemmli sample buffer.

Western blot analysis

For Western blot analysis the following primary antibodies were used: RhoA was identified using a mouse monoclonal IgG from Santa Cruz Biotechnologies (catalog number sc-418). Identification of C3 was achieved by a rabbit polyclonal antibody (affinity purified), which was raised against the full-length toxin C3bot (accession number CAA41767). ADP-ribosylated RhoA was detected by a specific antibody against ADP-ribosylated RhoA (ViF140_A1-hFc antibody was kindly provided by

Viola Fühner and Michael Hust, Technische Universität Braunschweig, Germany (22)). β-Actin was identified using mouse monoclonal anti-actin antibody (catalog number A5441, Sigma). Vimentin was identified using rabbit monoclonal anti-vimentin antibody (catalog number ab92547, Abcam, Cambridge, UK). α-Penta-His (catalog number 34660, Qiagen, Hilden, Germany) antibody was used to detect His-tagged vimentin. Western blot analyses were performed as described previously (23).

C3 overlay assay

35 μg of recombinant vimentin were separated by 15% SDS-PAGE and transferred to nitrocellulose membranes. After Western blot the transfer efficiency was checked with Ponceau S staining. After incubation with blocking buffer (5% powdered milk, in Tris-buffered saline with Tween (TBST)), membranes were probed with 10 μg/ml of purified C3 or C3-RGD mutants in blocking buffer 1 h at 4 °C. After extensive washing with TBST, membranes were incubated with C3 antibody, followed by HRP-conjugated secondary antibody (catalog number 611-1302, Rockland Immunochemicals Inc., Pottstown, PA), and detected by ECL. As a negative control, 2 μg/μl of BSA was loaded in the same nitrocellulose membranes and immunoblotted with C3 antibody. For the chemiluminescence reaction, ECL Femto (Pierce, Thermo Fisher Scientific Inc., Rockford, IL) or Immobilon (Millipore, Schwalbach, Germany) were used.

Vimentin overlay assay

4 μg of recombinant C3 protein were separated by native 15% PAGE and transferred to nitrocellulose membranes. After Western blot the transfer efficiency was checked with Ponceau S staining. After incubation with blocking buffer (5% powdered milk, in TBST), membranes were probed with 10 μg/ml of purified His-tagged vimentin in blocking buffer for 1 h at 4 °C. After extensive washing with TBST, membranes were incubated with C3 antibody or α-His, followed by HRP-conjugated secondary antibody, and detected by ECL. For the chemiluminescence reaction, ECL Femto (Pierce, Thermo Fisher Scientific Inc.) or Immobilon (Millipore, Schwalbach, Germany) were used. All signals were analyzed densitometrically using the KODAK 1D software (KODAK GmbH, Stuttgart, Germany).

Expression and purification of recombinant mouse vimentin proteins

Plasmids of mouse vimentins provided by Prof. Dr. Yi-Ling Li, Institute of Biomedical Sciences, Genomics Research Center, Academia Sinica, Taipei, Taiwan, were used (Liang *et al.* 55). The plasmids were transformed into BL21(DE3) cells. Induction was with 1 mM isopropyl 1-thio-β-D-galactopyranoside at 37 °C for 3 h. Recombinant vimentin proteins were purified as described by Machery-Nagel for His tag protein purification (Ni-IDA 2000 Packed Columns Protino, Machery-Nagel GmbH and Co. KG, Düren, Germany). Eluted proteins were analyzed by 15% SDS-PAGE, stained with Coomassie Blue, and submitted to Western blot analysis against α-penta-His (catalog number 34660, Qiagen, Hilden, Germany).

Reproducibility of the experiments and statistics

All experiments were performed independently at least three times. Results from representative experiments are shown in the figures. Graphs and statistical significance were calculated with GraphPad Prism software (version 6, GraphPad Software, Inc., San Diego, CA). When significant differences were found using ANOVA, Dunnett's multiple *t* test was used to compare the control (C3-treated cells) with the other groups (C3-G89I-treated cells, C3-D90G-treated cells, and C3-D90N-treated cells). The statistical significance of differences between treated vimentin-knock-out and wild-type neurons were calculated by the use of a two-sided unpaired Student's *t* test. Values ($n \geq 3$) are mean ± S.D. Differences were considered to be statistically significant at $p \leq 0.05$ (* = $p \leq 0.05$, ** = $p \leq 0.01$, and *** = $p \leq 0.001$).

Author contributions—I. J., A. R., M. H., and G. A. H. conceived and designed the experiments; S. H., A. A., E. O., and A. R. performed the experiments; A. R. and M. H. analyzed the data; I. J., A. R., M. H., and G. A. H. contributed reagents, materials, and analysis tools; A. R., I. J., M. H., and G. A. H. wrote the paper.

References

1. Aktories, K., Rösener, S., Blaschke, U., and Chhatwal, G. S. (1988) Botulinum ADP-ribosyltransferase C3: purification of the enzyme and characterization of the ADP-ribosylation reaction in platelet membranes. *Eur. J. Biochem.* **172,** 445–450
2. Popoff, M. R., Hauser, D., Boquet, P., Eklund, M. W., and Gill, D. M. (1991) Characterization of the C3 gene of *Clostridium botulinum* types C and D and its expression in *Escherichia coli*. *Infect. Immun.* **59,** 3673–3679
3. Just, I., Mohr, C., Schallehn, G., Menard, L., Didsbury, J. R., Vandekerckhove, J., van Damme, J., and Aktories, K. (1992) Purification and characterization of an ADP-ribosyltransferase produced by *Clostridium limosum*. *J. Biol. Chem.* **267,** 10274–10280
4. Just, I., Selzer, J., Jung, M., van Damme, J., Vandekerckhove, J., and Aktories, K. (1995) Rho-ADP-ribosylating exoenzyme from *Bacillus cereus:* purification, characterization, and identification of the NAD-binding site. *Biochemistry* **34,** 334–340
5. Inoue, S., Sugai, M., Murooka, Y., Paik, S. Y., Hong, Y. M., Ohgai, H., and Suginaka, H. (1991) Molecular cloning and sequencing of the epidermal cell differentiation inhibitor gene from *Staphylococcus aureus*. *Biochem. Biophys. Res. Commun.* **174,** 459–464
6. Wilde, C., Chhatwal, G. S., Schmalzing, G., Aktories, K., and Just, I. (2001) A novel C3-like ADP-ribosyltransferase from *Staphylococcus aureus* modifying RhoE and Rnd3. *J. Biol. Chem.* **276,** 9537–9542
7. Krska, D., Ravulapalli, R., Fieldhouse, R. J., Lugo, M. R., and Merrill, A. R. (2015) C3 larvin toxin, an ADP-ribosyltransferase from *Paenibacillus larvae*. *J. Biol. Chem.* **290,** 1639–1653
8. Aktories, K., and Just, I. (2005) Clostridial Rho-inhibiting protein toxins. *Curr. Top. Microbiol. Immunol.* **291,** 113–145
9. Sekine, A., Fujiwara, M., and Narumiya, S. (1989) Asparagine residue in the *rho* gene product is the modification site for botulinum ADP-ribosyltransferase. *J. Biol. Chem.* **264,** 8602–8605
10. Han, S., Arvai, A. S., Clancy, S. B., and Tainer, J. A. (2001) Crystal structure and novel recognition motif of rho ADP-ribosylating C3 exoenzyme from *Clostridium botulinum*: structural insights for recognition specificity and catalysis. *J. Mol. Biol.* **305,** 95–107
11. Toda, A., Tsurumura, T., Yoshida, T., Tsumori, Y., and Tsuge, H. (2015) Rho GTPase recognition by C3 exoenzyme based on C3-RhoA complex structure. *J. Biol. Chem.* **290,** 19423–19432
12. Aktories, K., Schmidt, G., and Just, I. (2000) Rho GTPases as targets of bacterial protein toxins. *Biol. Chem.* **381,** 421–426

13. Vogelsgesang, M., Pautsch, A., and Aktories, K. (2007) C3 exoenzymes, novel insights into structure and action of Rho-ADP-ribosylating toxins. *Naunyn. Schmiedebergs Arch. Pharmacol.* **374,** 347–360
14. Aullo, P., Giry, M., Olsnes, S., Popoff, M. R., Kocks, C., and Boquet, P. (1993) A chimeric toxin to study the role of the 21 kDa GTP binding protein rho in the control of actin microfilament assembly. *EMBO J.* **12,** 921–931
15. Barth, H., Hofmann, F., Olenik, C., Just, I., and Aktories, K. (1998) The N-terminal part of the enzyme component (C2I) of the binary *Clostridium botulinum* C2 toxin interacts with the binding component C2II and functions as a carrier system for a Rho ADP-ribosylating C3-like fusion toxine. *Infect. Immun.* **66,** 1364–1369
16. Sahai, E., and Olson, M. F. (2006) Purification of TAT-C3 exoenzyme. *Methods Enzymol.* **406,** 128–140
17. Ahnert-Hilger, G., Höltje, M., Grosse, G., Pickert, G., Mucke, C., Nixdorf-Bergweiler, B., Boquet, P., Hofmann, F., and Just, I. (2004) Differential effects of Rho GTPases on axonal and dendritic development in hippocampal neurones. *J. Neurochem.* **90,** 9–18
18. Höltje, M., Hoffmann, A., Hofmann, F., Mucke, C., Grosse, G., Van Rooijen, N., Kettenmann, H., Just, I., and Ahnert-Hilger, G. (2005) Role of Rho GTPase in astrocyte morphology and migratory response during *in vitro* wound healing. *J. Neurochem.* **95,** 1237–1248
19. Fahrer, J., Kuban, J., Heine, K., Rupps, G., Kaiser, E., Felder, E., Benz, R., and Barth, H. (2010) Selective and specific internalization of clostridial C3 ADP-ribosyltransferases into macrophages and monocytes. *Cell Microbiol.* **12,** 233–247
20. Rotsch, J., Rohrbeck, A., May, M., Kolbe, T., Hagemann, S., Schelle, I., Just, I., Genth, H., and Huelsenbeck, S. C. (2012) Inhibition of macrophage migration by *C. botulinum* exoenzyme C3. *Naunyn. Schmiedebergs Arch. Pharmacol.* **385,** 883–890
21. Rohrbeck, A., von Elsner, L., Hagemann, S., and Just, I. (2015) Uptake of *Clostridium botulinum* C3 exoenzyme into intact HT22 and J774A.1 cells. *Toxins* **7,** 380–395
22. Rohrbeck, A., Fühner, V., Schröder, A., Hagemann, S., Vu, X.-K., Berndt, S., Hust, M., Pich, A., and Just, I. (2016) Detection and quantification of ADP-ribosylated RhoA/B by monoclonal antibody. *Toxins* **8,** 100
23. Rohrbeck, A., Schröder, A., Hagemann, S., Pich, A., Höltje, M., Ahnert-Hilger, G., and Just, I. (2014) Vimentin mediates uptake of C3 exoenzyme. *PLoS ONE* **9,** e101071–e101071
24. Hynes, R. O. (1992) Integrins: versatility, modulation, and signaling in cell adhesion. *Cell.* **69,** 11–25
25. Humphries, J. D., Byron, A., and Humphries, M. J. (2006) Integrin ligands at a glance. *J. Cell Sci.* **119,** 3901–3903
26. Lee, W., Sodek, J., and McCulloch, C. A. (1996) Role of integrins in regulation of collagen phagocytosis by human fibroblasts. *J. Cell. Physiol.* **168,** 695–704
27. Bowditch, R. D., Halloran, C. E., Aota, S., Obara, M., Plow, E. F., Yamada, K. M., and Ginsberg, M. H. (1991) Integrin αIIbβ3 (platelet GPIIb-IIIa) recognizes multiple sites in fibronectin. *J. Biol. Chem.* **266,** 23323–23328
28. Reinholt, F. P., Hultenby, K., Oldberg, A., and Heinegård, D. (1990) Osteopontin: a possible anchor of osteoclasts to bone. *Proc. Natl. Acad. Sci. U.S.A.* **87,** 4473–4475
29. Barillari, G., Gendelman, R., Gallo, R. C., and Ensoli, B. (1993) The Tat protein of human immunodeficiency virus type 1, a growth factor for AIDS Kaposi sarcoma and cytokine-activated vascular cells, induces adhesion of the same cell types by using integrin receptors recognizing the RGD amino acid sequence. *Proc. Natl. Acad. Sci. U.S.A.* **90,** 7941–7945
30. Van Nhieu, G. T., and Isberg, R. R. (1991) The *Yersinia pseudotuberculosis* invasin protein and human fibronectin bind to mutually exclusive sites on the α5β1 integrin receptor. *J. Biol. Chem.* **266,** 24367–24375
31. Khan, T. A., Wang, X., and Maynard, J. A. (2016) Inclusion of an RGD motif alters invasin integrin-binding affinity and specificity. *Biochemistry* **55,** 2078–2090
32. Parry, C., Bell, S., Minson, T., and Browne, H. (2005) Herpes simplex virus type 1 glycoprotein H binds to αvβ3 integrins. *J. Gen. Virol.* **86,** 7–10
33. Chesnokova, L. S., Nishimura, S. L., and Hutt-Fletcher, L. M. (2009) Fusion of epithelial cells by Epstein-Barr virus proteins is triggered by binding of viral glycoproteins gHgL to integrins αvβ6 or αvβ8. *Proc. Natl. Acad. Sci. U.S.A.* **106,** 20464–20469
34. Feire, A. L., Koss, H., and Compton, T. (2004) Cellular integrins function as entry receptors for human cytomegalovirus via a highly conserved disintegrin-like domain. *Proc. Natl. Acad. Sci. U.S.A.* **101,** 15470–15475
35. Giannone, G., Jiang, G., Sutton, D. H., Critchley, D. R., and Sheetz, M. P. (2003) Talin1 is critical for force-dependent reinforcement of initial integrin-cytoskeleton bonds but not tyrosine kinase activation. *J. Cell Biol.* **163,** 409–419
36. Kiema, T., Lad, Y., Jiang, P., Oxley, C. L., Baldassarre, M., Wegener, K. L., Campbell, I. D., Ylänne, J., and Calderwood, D. A. (2006) The molecular basis of filamin binding to integrins and competition with talin. *Mol. Cell.* **21,** 337–347
37. Loo, D. T., Kanner, S. B., and Aruffo, A. (1998) Filamin binds to the cytoplasmic domain of the β1-integrin: identification of amino acids responsible for this interaction. *J. Biol. Chem.* **273,** 23304–23312
38. Calderwood, D. A., Huttenlocher, A., Kiosses, W. B., Rose, D. M., Woodside, D. G., Schwartz, M. A., and Ginsberg, M. H. (2001) Increased filamin binding to β-integrin cytoplasmic domains inhibits cell migration. *Nat. Cell Biol.* **3,** 1060–1068
39. Gehler, S., Baldassarre, M., Lad, Y., Leight, J. L., Wozniak, M. A., Riching, K. M., Eliceiri, K. W., Weaver, V. M., Calderwood, D. A., and Keely, P. J. (2009) Filamin A–β1 integrin complex tunes epithelial cell response to matrix tension. *Mol. Biol. Cell* **20,** 3224–3238
40. Homan, S. M., Mercurio, A. M., and LaFlamme, S. E. (1998) Endothelial cells assemble two distinct α6β4-containing vimentin-associated structures: roles for ligand binding and the β4 cytoplasmic tail. *J. Cell Sci.* **111,** 2717–2728
41. Wang, X. Q., and Frazier, W. (1998) The thrombospondin receptor CD47 (IAP) modulates and associates with α2β1 integrin in vascular smooth muscle cells. *Mol. Biol. Cell.* **9,** 865–874
42. Gonzales, M., Weksler, B., Tsuruta, D., Goldman, R. D., Yoon, K. J., Hopkinson, S. B., Flitney, F. W., and Jones, J. C. (2001) Structure and function of a vimentin-associated matrix adhesion in endothelial cells. *Mol. Biol. Cell.* **12,** 85–100
43. Kreis, S., Schönfeld, H. J., Melchior, C., Steiner, B., and Kieffer, N. (2005) The intermediate filament protein vimentin binds specifically to a recombinant integrin α2/β1 cytoplasmic tail complex and co-localizes with native α2/β1 in endothelial cell focal adhesions. *Exp. Cell Res.* **305,** 110–121
44. Kim, J., Yang, C., Kim, E. J., Jang, J., Kim, S. J., Kang, S. M., Kim, M. G., Jung, H., Park, D., and Kim, C. (2016) Vimentin filaments regulate integrin-ligand interactions by binding to the cytoplasmic tail of integrin β3. *J. Cell Sci.* **129,** 2030–2042
45. Bhattacharya, R., Gonzalez, A. M., Debiase, P. J., Trejo, H. E., Goldman, R. D., Flitney, F. W., and Jones, J. C. (2009) Recruitment of vimentin to the cell surface by β3 integrin and plectin mediates adhesion strength. *J. Cell Sci.* **122,** 1390–1400
46. Gilles, C., Polette, M., Zahm, J. M., Tournier, J. M., Volders, L., Foidart, J. M., and Birembaut, P. (1999) Vimentin contributes to human mammary epithelial cell migration. *J. Cell Sci.* **112,** 4615–4625
47. Nieminen, M., Henttinen, T., Merinen, M., Marttila-Ichihara, F., Eriksson, J. E., and Jalkanen, S. (2006) Vimentin function in lymphocyte adhesion and transcellular migration. *Nat. Cell Biol.* **8,** 156–162
48. Satelli, A., and Li, S. (2011) Vimentin in cancer and its potential as a molecular target for cancer therapy. *Cell. Mol. Life Sci.* **68,** 3033–3046
49. Eckes, B., Colucci-Guyon, E., Smola, H., Nodder, S., Babinet, C., Krieg, T., and Martin, P. (2000) Impaired wound healing in embryonic and adult mice lacking vimentin. *J. Cell Sci.* **113,** 2455–2462
50. Chang, I. A., Oh, M. J., Kim, M. H., Park, S. K., Kim, B. G., and Namgung, U. (2012) Vimentin phosphorylation by Cdc2 in Schwann cell controls axon growth via 1-integrin activation. *FASEB J.* **26,** 2401–2413
51. Garg, A., Barnes, P. F., Porgador, A., Roy, S., Wu, S., Nanda, J. S., Griffith, D. E., Girard, W. M., Rawal, N., Shetty, S., and Vankayalapati, R. (2006) Vimentin expressed on *Mycobacterium tuberculosis*-infected human monocytes is involved in binding to the NKp46 receptor. *J. Immunol.* **177,** 6192–6198

52. Kim, J.-K., Fahad, A.-M., Shanmukhappa, K., and Kapil, S. (2006) Defining the cellular target(s) of porcine reproductive and respiratory syndrome virus blocking monoclonal antibody 7G10. *J. Virol.* **80,** 689–696
53. Koudelka, K. J., Destito, G., Plummer, E. M., Trauger, S. A., Siuzdak, G., and Manchester, M. (2009) Endothelial targeting of cowpea mosaic virus (CPMV) via surface vimentin. *PLoS Pathog.* **5,** e1000417
54. Das, S., Ravi, V., and Desai, A. (2011) Japanese encephalitis virus interacts with vimentin to facilitate its entry into porcine kidney cell line. *Virus Res.* **160,** 404–408
55. Liang, J. J., Yu, C. Y., Liao, C. L., and Lin, Y. L. (2011) Vimentin binding is critical for infection by the virulent strain of Japanese encephalitis virus. *Cell. Microbiol.* **13,** 1358–1370
56. Yu, Y. T., Chien, S. C., Chen, I. Y., Lai, C. T., Tsay, Y. G., Chang, S. C., and Chang, M. F. (2016) Surface vimentin is critical for the cell entry of SARS-CoV. *J. Biomed Sci.* 10.1186/s12929–016-0234–7
57. Esue, O., Carson, A. A., Tseng, Y., and Wirtz, D. (2006) A direct interaction between actin and vimentin filaments mediated by the tail domain of vimentin. *J. Biol. Chem.* **281,** 30393–30399
58. Bocquet, A., Berges, R., Frank, R., Robert, P., Peterson, A. C., and Eyer, J. (2009) Neurofilaments bind tubulin and modulate its polymerization. *J. Neurosci.* **29,** 11043–11054
59. Robert, A., Herrmann, H., Davidson, M. W., and Gelfand, V. I. (2014) Microtubule-dependent transport of vimentin filament precursors is regulated by actin and by the concerted action of Rho- and p21-activated kinases. *FASEB J.* **28,** 2879–2890
60. Kim, H., Nakamura, F., Lee, W., Shifrin, Y., Arora, P., and McCulloch, C. (2010) Filamin A is required for vimentin-mediated cell adhesion and spreading. *Am. J. Physiol. Cell Physiol.* **298,** C221–C236
61. Päll, T., Pink, A., Kasak, L., Turkina, M., Anderson, W., Valkna, A., and Kogerman, P. (2011) Soluble CD44 interacts with intermediate filament protein vimentin on endothelial cell surface. *PLoS ONE* **6,** e29305
62. Shigyo, M., Kuboyama, T., Sawai, Y., Tada-Umezaki, M., and Tohda, C. (2015) Extracellular vimentin interacts with insulin-like growth factor 1 receptor to promote axonal growth. *Sci. Rep.* **5,** 12055
63. Adolf, A., Leondaritis, G., Rohrbeck, A., Eickholt, B. J., Just, I., Ahnert-Hilger, G., and Höltje, M. (2016) The intermediate filament protein vimentin is essential for axonotrophic effects of *Clostridium botulinum* C3 exoenzyme. *J. Neurochem.* **139,** 234–244
64. Holbourn, K. P., Shone, C. C., and Acharya, K. R. (2006) A family of killer toxins: exploring the mechanism of ADP-ribosylating toxins. *FEBS J.* **273,** 4579–4593
65. Ruoslahti, E. (1996) Rgd and other recognition sequences for integrins. *Annu. Rev. Cell Dev. Biol.* **12,** 697–715
66. Hermosilla, T., Muñoz, D., Herrera-Molina, R., Valdivia, A., Muñoz, N., Nham, S. U., Schneider, P., Burridge, K., Quest, A. F., and Leyton, L. (2008) Direct Thy-1/αVβ3 integrin interaction mediates neuron to astrocyte communication. *Biochim Biophys Acta.* **1783,** 1111–1120
67. Poncz, M., and Newman, P. J. (1990) Analysis of rodent platelet glycoprotein IIb: evidence for evolutionarily conserved domains and alternative proteolytic processing. *Blood* **75,** 1282–1289
68. Doray, B., and Kornfeld, S. (2001) Gamma subunit of the AP-1 adaptor complex binds clathrin: implications for cooperative binding in coated vesicle assembly. *Mol. Biol. Cell* **12,** 1925–1935
69. Jackson, T., Clark, S., Berryman, S., Burman, A., Cambier, S., Mu, D., Nishimura, S., and King, A. M. (2004) Integrin alphavbeta8 functions as a receptor for foot-and-mouth disease virus: role of the β-chain cytodomain in integrin-mediated infection. *J. Virol.* **78,** 4533–4540
70. Garrigues, H. J., Rubinchikova, Y. E., Dipersio, C. M., and Rose, T. M. (2008) Integrin αVβ3 binds to the RGD motif of glycoprotein B of Kaposi's sarcoma-associated herpesvirus and functions as an RGD-dependent entry receptor. *J. Virol.* **82,** 1570–1580
71. Gianni, T., Salvioli, S., Chesnokova, L. S., Hutt-Fletcher, L. M., and Campadelli-Fiume, G. (2013) αvβ6- and αvβ8-integrins serve as interchangeable receptors for HSV gH/gL to promote endocytosis and activation of membrane fusion. *PLoS Pathog.* **9,** e1003806
72. Walker, L. R., Hussein, H. A., and Akula, S. M. (2016) Subcellular fractionation method to study endosomal trafficking of Kaposi's sarcoma-associated herpesvirus. *Cell Biosci.* 10.1186/s13578–015-0066–2
73. Liang, X., and Ji, Y. (2006) α-Toxin interferes with integrin-mediated adhesion and internalization of *Staphylococcus aureus* by epithelial cells. *Cell. Microbiol.* **8,** 1656–1668
74. Stockbauer, K. E., Magoun, L., Liu, M., Burns, E. H., Jr., Gubba, S., Renish, S., Pan, X., Bodary, S. C., Baker, E., Coburn, J., Leong, J. M., and Musser, J. M. (1999) A natural variant of the cysteine protease virulence factor of group A *Streptococcus* with an arginine-glycine-aspartic acid (RGD) motif preferentially binds human integrins αvβ3 and αIIbβ3. *Proc. Natl. Acad. Sci. U.S.A.* **96,** 242–247
75. Altieri, D. C., Plescia, J., and Plow, E. F. (1993) The structural motif glycine 190-valine 202 of the fibrinogen γ chain interacts with CD11b/CD18 integrin (αM β2, Mac-1) and promotes leukocyte adhesion. *J. Biol. Chem.* **268,** 1847–1853
76. Podor, T. J., Singh, D., Chindemi, P., Foulon, D. M., McKelvie, R., Weitz, J. I., Austin, R., Boudreau, G., and Davies, R. (2002) Vimentin exposed on activated platelets and platelet microparticles localizes vitronectin and plasminogen activator inhibitor complexes on their surface. *J. Biol. Chem.* **277,** 7529–7539
77. Boilard, E., Bourgoin, S. G., Bernatchez, C., and Surette, M. E. (2003) Identification of an autoantigen on the surface of apoptotic human T cells as a new protein interacting with inflammatory group IIA phospholipase A 2. *Blood* **102,** 2901–2909
78. Xu, B., deWaal, R. M., Mor-Vaknin, N., Hibbard, C., Markovitz, D. M., and Kahn, M. L. (2004) The endothelial cell-specific antibody PAL-E identifies a secreted form of vimentin in the blood vasculature. *Mol. Cell. Biol.* **24,** 9198–9206
79. Moisan, E., and Girard, D. (2006) Cell surface expression of intermediate filament proteins vimentin and lamin B1 in human neutrophil spontaneous apoptosis. *J. Leukoc. Biol.* **79,** 489–498
80. Huet, D., Bagot, M., Loyaux, D., Capdevielle, J., Conraux, L., Ferrara, P., Bensussan, A., and Marie-Cardine, A. (2006) SC5 mAb represents a unique tool for the detection of extracellular vimentin as a specific marker of Sezary cells. *J. Immunol.* **176,** 652–659
81. Zou, Y., He, L., and Huang, S. H. (2006) Identification of a surface protein on human brain microvascular endothelial cells as vimentin interacting with *Escherichia coli* invasion protein IbeA. *Biochem. Biophys. Res. Commun.* **351,** 625–630
82. Mak, T., and Brüggemann, H. (2016) Vimentin in bacterial infections. *Cells* **5,** e18
83. Li, W., Moore, M. J., Vasilieva, N., Sui, J., Wong, S. K., Berne, M. A., Somasundaran, M., Sullivan, J. L., Luzuriaga, K., Greenough, T. C., Choe, H., and Farzan, M. (2003) Angiotensin-converting enzyme 2 is a functional receptor for the SARS coronavirus. *Nature* **426,** 450–454
84. Akula, S. M., Pramod, N. P., Wang, F. Z., and Chandran, B. (2002) Integrin α3β1 (CD 49c/29) is a cellular receptor for Kaposi's sarcoma-associated herpesvirus (KSHV/HHV-8) entry into the target cells. *Cell* **108,** 407–419
85. Hahn, A. S., Kaufmann, J. K., Wies, E., Naschberger, E., Panteleev-Ivlev, J., Schmidt, K., Holzer, A., Schmidt, M., Chen, J., König, S., Ensser, A., Myoung, J., Brockmeyer, N. H., Stürzl, M., Fleckenstein, B., and Neipel, F. (2012) The ephrin receptor tyrosine kinase A2 is a cellular receptor for Kaposi's sarcoma–associated herpesvirus. *Nat. Med.* **18,** 961–966
86. Walker, L. R., Hussein, H. A., and Akula, S. M. (2014) Disintegrin-like domain of glycoprotein B regulates Kaposi's sarcoma-associated herpesvirus infection of cells. *J. Gen. Virol.* **95,** 1770–1782
87. Bergelson, J. M., Cunningham, J. A., Droguett, G., Kurt-Jones, E. A., Krithivas, A., Hong, J. S., Horwitz, M. S., Crowell, R. L., and Finberg, R. W. (1997) Isolation of a common receptor for Coxsackie B viruses and adenoviruses 2 and 5. *Science* **275,** 1320–1323
88. Lütschg, V., Boucke, K., Hemmi, S., and Greber, U. F. (2011) Chemotactic antiviral cytokines promote infectious apical entry of human adenovirus into polarized epithelial cells. *Nat. Commun.* **2,** 391
89. Stencel-Baerenwald, J. E., Reiss, K., Reiter, D. M., Stehle, T., and Dermody, T. S. (2014) The sweet spot: defining virus–sialic acid interactions. *Nat. Rev. Microbiol.* **12,** 739–749
90. Maginnis, M. S., Forrest, J. C., Kopecky-Bromberg, S. A., Dickeson, S. K., Santoro, S. A., Zutter, M. M., Nemerow, G. R., Bergelson, J. M., and Der-

mody, T. S. (2006) β1 integrin mediates internalization of mammalian reovirus. *J. Virol.* **80,** 2760–2770
91. Barton, E. S., Forrest, J. C., Connolly, J. L., Chappell, J. D., Liu, Y., Schnell, F. J., Nusrat, A., Parkos, C. A., and Dermody, T. S. (2001) Junction adhesion molecule is a receptor for reovirus. *Cell* **104,** 441–451
92. Cera, M. R., Fabbri, M., Molendini, C., Corada, M., Orsenigo, F., Rehberg, M., Reichel, C. A., Krombach, F., Pardi, R., and Dejana, E. (2009) JAM-A promotes neutrophil chemotaxis by controlling integrin internalization and recycling. *J. Cell Sci.* **122,** 268–277
93. Yang, J., Zou, L., Yang, Y., Yuan, J., Hu, Z., Liu, H., Peng, H., Shang, W., Zhang, X., Zhu, J., and Rao, X. (2016) Superficial vimentin mediates DENV-2 infection of vascular endothelial cells. *Sci. Rep.* **6,** 38372
94. Zhang, J. L., Wang, J. L., Gao, N., Chen, Z. T., Tian, Y. P., and An, J. (2007) Up-regulated expression of beta3 integrin induced by dengue virus serotype 2 infection associated with virus entry into human dermal microvascular endothelial cells. *Biochem. Biophys. Res. Commun.* **356,** 763–768
95. Tobaben, S., Grohm, J., Seiler, A., Conrad, M., Plesnila, N., and Culmsee, C. (2011) Bid-mediated mitochondrial damage is a key mechanism in glutamate-induced oxidative stress and AIF-dependent cell death in immortalized HT-22 hippocampal neurons. *Cell Death Differ.* **18,** 282–292
96. Becher, A., Drenckhahn, A., Pahner, I., Margittai, M., Jahn, R., and Ahnert-Hilger, G. (1999) The synaptophysin-synaptobrevin complex: a hallmark of synaptic vesicle maturation. *J Neurosci.* **19,** 1922–1931